JCTC Journal of Chemical Theory and Computation

Article

Cite This: J. Chem. Theory Comput. 2018, 14, 2034−2041

pubs.acs.org/JCTC

A Well-Tempered Hybrid Method for Solving Challenging Time-Dependent Density Functional Theory (TDDFT) Systems

Joseph M. Kasper,[†] David B. Williams-Young,[†] Eugene Vecharynski,[‡] Chao Yang,[‡] and Xiaosong Li*[,†]

[†]Department of Chemistry, University of Washington, Seattle, Washington 98195, United States

[‡]Computational Research Division, Lawrence Berkeley National Laboratory, Berkeley, California 94720, United States

Supporting Information

ABSTRACT: The time-dependent Hartree−Fock (TDHF) and time-dependent density functional theory (TDDFT) equations allow one to probe electronic resonances of a system quickly and inexpensively. However, the iterative solution of the eigenvalue problem can be challenging or impossible to converge, using standard methods such as the Davidson algorithm for spectrally dense regions in the interior of the spectrum, as are common in X-ray absorption spectroscopy (XAS). More robust solvers, such as the generalized preconditioned locally harmonic residual (GPLHR) method, can alleviate this problem, but at the expense of higher average computational cost. A hybrid method is proposed which adapts to the problem in order to maximize computational performance while providing the superior convergence of GPLHR. In addition, a modification to the GPLHR algorithm is proposed to adaptively choose the shift parameter to enforce a convergence of states above a predefined energy threshold.

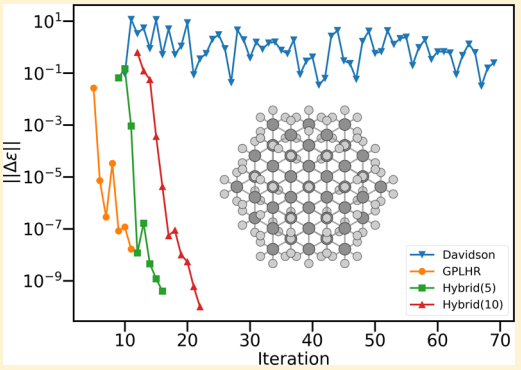

1. INTRODUCTION

The computation of electronic excited states plays a very important role in understanding the response of molecular and material systems to external electromagnetic perturbations. Linear-response time-dependent density functional theory (LR-TDDFT)[1−3] is one of the most popular methods for this purpose, because of its excellent balance between accuracy and computational cost. Although LR-TDDFT is among the most tractable methods for excited-state calculations, it still leverages a large computational demand for large molecular systems, such as those of photochemical interest. The computational cost of solving the TDDFT equations using iterative techniques, such as the Davidson algorithm,[4−6] formally scales as $O(MN^4)$, where N is the total number of basis functions and M is the number of excited states sought. With the development of efficient linear-scaling methods for direct formation of Fock/Kohn−Sham-like operators, the scaling of conventional implementations of LR-TDDFT may be reduced to $O(MN^2) - O(MN^3)$ in complexity.[7] While efficient implementations of LR-TDDFT[8−10] are routinely used to to obtain characteristics of lowest-lying molecular excited states, modifications to the Davidson algorithm such as energy-specific windowing[11−13] or restricted excitation windowing[14−16] have also been used to resolve the spectral interior of the LR-TDDFT equation, which is crucial to modeling K-edge X-ray absorption spectroscopy (XAS).

However, for systems that exhibit a dense manifold of excited states in the spectral region of interest, e.g., carbon K-edge XAS of a nanographene or a nanodiamond, solving the LR-TDDFT equations by iterative diagonalization is still very expensive and subject to nontrivial convergence problems. While alternatives to diagonalization have also been explored, including frequency dependent-response[17−24] and model order reduction,[25,26] the eigenvector approach provides easy interpretation in the context of electronic adiabats.[27] Recently, more robust methods have been proposed for non-Hermitian eigenvalue problems such as the generalized preconditioned locally harmonic residual (GPLHR) algorithm.[28] This solver can reliably converge the closest N roots to a specified spectral shift for arbitrary complex matrices. Its use in chemistry has proven to be effective for EOM-CCSD calculations, although an increased average computational cost over the Davidson algorithm is traded for improved convergence characteristics.[29]

In this work, we introduce a modified energy-specific GPLHR method and a well-tempered hybrid method of Davidson and GPLHR methods for solving challenging TDDFT systems. This method takes advantage of the benefits of different iterative diagonalizers, using a hybrid scheme incorporating an adaptive switching between both energy-specific Davidson and GPLHR. We report the results on a variety of test systems in the very challenging high-energy X-ray

Received: February 7, 2018
Published: March 16, 2018

DOI: 10.1021/acs.jctc.8b00141
J. Chem. Theory Comput. 2018, 14, 2034−2041

region with dense manifolds of excited states. In addition to providing additional robustness of convergence for systems for which the Davidson algorithm fails, we find that there are systems where a hybrid approach is able to computationally beat the use of either method alone.

2. THEORY

Because the formalism of the linear response TDHF/TDDFT is a well-established method, we only present a brief review herein. For a detailed discussion, we refer the interested reader to ref 10. The linear response of a molecular system subject to perturbation by an external electromagnetic field is given by the TDHF or TDDFT equations

$$\begin{pmatrix} \mathbf{A} & \mathbf{B} \\ \mathbf{B}^* & \mathbf{A}^* \end{pmatrix} \begin{pmatrix} \mathbf{X} \\ \mathbf{Y} \end{pmatrix} = E \begin{pmatrix} 1 & 0 \\ 0 & -1 \end{pmatrix} \begin{pmatrix} \mathbf{X} \\ \mathbf{Y} \end{pmatrix} \tag{1}$$

where the matrices $\mathbf{A}$ and $\mathbf{B}$ for TDHF are defined as

$$A_{ai,bj} = \delta_{ab}\delta_{ij}(\epsilon_a - \epsilon_i) + (ia|jb) - (ib|ja) \tag{2}$$

$$B_{ai,bj} = (ia|bj) - (ij|ba) \tag{3}$$

and for TDDFT as

$$A_{ai,bj} = \delta_{ab}\delta_{ij}(\epsilon_a - \epsilon_i) + (ia|jb) - \alpha(ib|ja) + (ia|f_{xc}|jb) \tag{4}$$

$$B_{ai,bj} = (ia|bj) - \alpha(ij|ba) + (ia|f_{xc}|bj) \tag{5}$$

The two electron integrals have been expressed in the canonical molecular orbital (MO) basis in Mulliken notation where i and j indices are used for occupied MOs and a and b indices for virtual MOs, ϵ_p is the orbital energy of the Kohn−Sham operator for MO p, and α is a real scaling parameter such that, for pure DFT kernels, $\alpha = 0$, whereas, for hybrid DFT, the scaling factor α determines the fraction of Hartree−Fock exchange to be included. The eigensystem of eq 1 describes the electronic adiabatic states of the molecular system with the eigenvalues corresponding to the electronic resonances (excitation energies) of the system, while the corresponding eigenvectors describe the orbital excitation and de-excitation amplitudes for the adiabat. In the case of real-valued matrices, $\mathbf{A}^* = \mathbf{A}$ and $\mathbf{B}^* = \mathbf{B}$, so one can also solve the equivalent problem of half the dimension:[5,8,30]

$$(\mathbf{A} - \mathbf{B})(\mathbf{A} + \mathbf{B})|\mathbf{X} + \mathbf{Y}\rangle = \omega^2|\mathbf{X} + \mathbf{Y}\rangle \tag{6}$$

2.1. Davidson-like Methods. For many systems of chemical interest, the dimension of the matrices is far too large to store in memory for full diagonalization and must be partially diagonalized by iterative methods. One of the most well-known methods for iterative diagonalization of the CIS equations was proposed by Davidson in 1975.[4] Modifications have allowed it to be extended to the RPA equations,[5,6,8,31] as well as providing restricted excitation[14−16] or energy-specific windowing[11,13] to obtain higher-energy roots. The following is a basic overview of the energy-specific algorithm used here, but for a detailed implementation of the Davidson algorithm for solving the RPA equations, we invite the reader to see refs 11 or 32.

The basic idea of the Davidson algorithm is to work in a much smaller reduced dimensional search space and find the best approximate (right) eigenvectors for eq 6 as a linear combination of basis vectors $|\mathbf{b}_i\rangle$:

$$|\mathbf{X}_j + \mathbf{Y}_j\rangle = \sum_{i=1}^{m} c_{ij}|\mathbf{b}_i\rangle \tag{7}$$

where the coefficients c_{ij} are found by diagonalization of the subspace problem. To do this, the action of the $(\mathbf{A}+\mathbf{B})$ and $(\mathbf{A}-\mathbf{B})$ matrices on the $\mathbf{b}_i$ vectors is calculated directly. Stratmann et al.[8] then noted that, in the limit of convergence, $\langle \mathbf{b}_i|(\mathbf{A}-\mathbf{B})(\mathbf{A}+\mathbf{B})|\mathbf{b}_j\rangle$ will have the same solutions as

$$\tilde{M}_{ij} = \sum_k \langle \mathbf{b}_i|\mathbf{A}-\mathbf{B}|\mathbf{b}_k\rangle\langle \mathbf{b}_k|\mathbf{A}+\mathbf{B}|\mathbf{b}_j\rangle \tag{8}$$

This non-Hermitian matrix product is diagonalized to determine the best approximate right and left eigenvectors $|\tilde{\mathbf{R}}\rangle$, $|\tilde{\mathbf{L}}\rangle$, and the corresponding eigenvalues $\tilde{\omega}$ in the subspace. The eigenvectors contain the coefficients to transform $|\tilde{\mathbf{R}}\rangle$ and $|\tilde{\mathbf{L}}\rangle$ from the reduced space to the full MO space ($|\mathbf{R}\rangle$, $|\mathbf{L}\rangle$). In the energy-specific case, we choose to transform the first n eigenvectors with $\tilde{\omega}_i \geq \omega_0$, where ω_0 is the energy threshold. Otherwise, one can take $\omega_0 = 0$ and transform the n lowest energy roots.

To determine if the approximation is good enough, the left and right components of the residual vectors $|\mathbf{W}_n\rangle$ are given by

$$|\mathbf{W}_n^{\mathrm{L}}\rangle = (\mathbf{A}+\mathbf{B})|\mathbf{R}_n\rangle - \tilde{\omega}_n|\mathbf{L}_n\rangle \tag{9}$$

and

$$|\mathbf{W}_n^{\mathrm{R}}\rangle = (\mathbf{A}-\mathbf{B})|\mathbf{L}_n\rangle - \tilde{\omega}_n|\mathbf{R}_n\rangle \tag{10}$$

If the residuals are nonzero, new vectors are constructed and added to the subspace. While the residual vectors could be added to the set of $|\mathbf{b}_i\rangle$ without further modification, it is more efficient to use a preconditioner to achieve quasi-second-order information. Since the left-hand side of eq 1 is diagonally dominant with the orbital energy differences, the preconditioned residual vectors are given by

$$Q_{\mathrm{in}} = (\tilde{\omega}_n - \Delta\epsilon)^{-1}W_{in} \tag{11}$$

Here, the $\Delta\epsilon$ term represents the orbital energy differences along the diagonal of $\mathbf{A}$. These $\mathbf{Q}$ vectors are added to the set of existing $\mathbf{b}$, and the entire process is repeated until the norm of the residuals falls below a specified threshold (or equivalently that $\tilde{\omega}_i$ stop changing) and convergence is achieved. As the number of basis vectors $\mathbf{b}_i$ approaches the full dimension of the matrix, the approximation greatly approaches the exact solution. However, it is also possible that the number of $\mathbf{b}_i$ grows very large before convergence, in which case the algorithm can be restarted by collapsing the subspace down to a small number of vectors, using the best $|\mathbf{R}\rangle$ and $|\mathbf{L}\rangle$.

2.2. The GPLHR Method for Obtaining High-Energy Excited States. The GPLHR algorithm is a recently proposed method[28] to iteratively solve the generalized eigenvalue problem for arbitrary non-Hermitian square matrices $\mathcal{H}$ and $\mathcal{M}$:

$$\mathcal{H}|\mathbf{x}\rangle = \omega\mathcal{M}|\mathbf{x}\rangle \tag{12}$$

Note that, in the context of eq 1, $\mathcal{H}$ and $\mathcal{M}$ are represented here in the full dimension problem and not the half-dimension problem in eq 6, as are all other quantities in calligraphic script font.

In particular, GPLHR aims to improve the convergence and performance of iterative diagonalization for a targeted region in the interior of the spectrum. That is, given some target shift σ, GPLHR attempts to find the n eigenvalues ω_i closest to σ along

DOI: 10.1021/acs.jctc.8b00141
J. Chem. Theory Comput. 2018, 14, 2034−2041

with the associated eigenvectors $|\mathbf{x}_i\rangle$. We also note here that, unlike the strict lower-bound ω_0 used in energy-specific Davidson algorithm, we obtain the closest values to σ both above *and* below.

An excellent technical report of the GPLHR algorithm is published elsewhere,[28] to which we refer interested readers. Here, we provide an overview of the salient points to facilitate comparison with the Davidson and Lanczos families of algorithms, as well as how these two methods can complement each other in an adaptive hybrid scheme for the TDHF/TDDFT problem.

First, given some set of orthonormalized initial guess (right) vectors $\mathcal{V}$, we form the set of vectors $\mathcal{Q}$ in the σ-shifted space, according to

$$\mathcal{Q} = (\mathcal{H} - \sigma\mathcal{M})\mathcal{V} \tag{13}$$

followed by orthonormalization. The generalized eigenproblem

$$(\mathcal{Q}^\dagger\mathcal{H}\mathcal{V}, \mathcal{Q}^\dagger\mathcal{M}\mathcal{V}) \tag{14}$$

can then be solved to obtain initial approximations for $\tilde{\omega}_i$. Since $\mathcal{Q}$ is in the σ-shifted space, we obtain a better approximate $\tilde{\omega}_i$ near σ through the harmonic Rayleigh-Ritz procedure.

Although eq 14 can be solved by diagonalization-based methods, we instead use generalized Schur decomposition (also known as QZ factorization), which has the advantage of being well-defined for any two matrices. From the Schur decomposition of eq 14, we obtain the triangular factors $\mathcal{R}_1$, $\mathcal{R}_2$, as well as Schur bases $\mathcal{Y}_\mathrm{L}$, $\mathcal{Y}_\mathrm{R}$, such that

$$\mathcal{Q}^\dagger\mathcal{H}\mathcal{V} = \mathcal{Y}_\mathrm{L}\mathcal{R}_1\mathcal{Y}_\mathrm{R} \tag{15}$$

and

$$\mathcal{Q}^\dagger\mathcal{M}\mathcal{V} = \mathcal{Y}_\mathrm{L}\mathcal{R}_2\mathcal{Y}_\mathrm{R} \tag{16}$$

The eigenvalues are given by the ratio of the diagonal elements of the triangular factors:

$$\omega_j = \frac{\mathcal{R}_1(j,j)}{\mathcal{R}_2(j,j)} \tag{17}$$

The Schur vectors $\mathcal{Y}_\mathrm{L}$ and $\mathcal{Y}_\mathrm{R}$ can be used to update $\mathcal{V}$ and $\mathcal{Q}$, with $\mathcal{V} \to \mathcal{V}\mathcal{Y}_\mathrm{R}$ and $\mathcal{Q} \to \mathcal{Q}\mathcal{Y}_\mathrm{L}$. More importantly, we can use the information in the triangular factors in the process of generating new vectors to form a new test subspace and generalized eigenproblem.

In contrast to the Davidson algorithm, in which the subspace grows at each iteration, GPLHR generates a subspace of fixed size based on an integer parameter m. This is used to update the current solution $\mathcal{V}$ but is discarded and not reused on subsequent iterations. This trial subspace $\mathcal{Z} = [\mathcal{V}, \mathcal{W}, \mathcal{S}_1, ..., \mathcal{S}_m, \mathcal{P}]$ corresponds to the Krylov–Arnoldi sequence generated by the preconditioned residuals and is constructed as shown in Algorithm 1.

Algorithm 1: Generation of Trial Subspace

Input : Vectors $\mathcal{V}$, Schur factors $\mathcal{R}_1$, $\mathcal{R}_2$, preconditioner $\mathcal{T}$, and approximate eigenvalues $\tilde{\omega}$
Output: Krylov-Arnoldi sequence $[\mathcal{W}, \mathcal{S}_1, ..., \mathcal{S}_m]$
Form diagonal matrices $\mathcal{G}_1$ and $\mathcal{G}_2$ by Eq. (18) and Eq. (19)
$\mathcal{G} \leftarrow \mathcal{R}_1\mathcal{G}_1 + \mathcal{R}_2\mathcal{G}_2$
$\mathcal{B}_1 \leftarrow \mathcal{G}_2\mathcal{G}^{-1}\mathcal{R}_1; \mathcal{B}_2 \leftarrow \mathcal{I} - \mathcal{G}_1\mathcal{G}^{-1}\mathcal{R}_1$
$\mathcal{W} \leftarrow (\mathcal{I} - \mathcal{V}\mathcal{V}^\dagger)\mathcal{T}(\mathcal{I} - \mathcal{Q}\mathcal{Q}^\dagger)(\mathcal{H}\mathcal{V}\mathcal{B}_2 - \mathcal{M}\mathcal{V}\mathcal{B}_1)$
Set $\mathcal{S}_0 \leftarrow \mathcal{W}$
for $l = 1, \ldots, m$ **do**
  $\mathcal{S}_l \leftarrow (\mathcal{I} - \mathcal{V}\mathcal{V}^\dagger)\mathcal{T}(\mathcal{I} - \mathcal{Q}\mathcal{Q}^\dagger)(\mathcal{H}\mathcal{S}_{l-1}\mathcal{B}_2 - \mathcal{M}\mathcal{S}_{l-1}\mathcal{B}_1)$
end

$\mathcal{P}$ is an additional block of saved vectors and is not used on the first iteration. The matrices $\mathcal{G}_1$ and $\mathcal{G}_2$ are diagonal and constructed from the triangular factors $\mathcal{R}_1$ and $\mathcal{R}_2$ as follows:

$$\mathcal{G}_1(j,j) = \begin{cases} 0 & |\mathcal{R}_1(j,j)| < |\mathcal{R}_2(j,j)| \\ \dfrac{1 - \mathcal{R}_2(j,j)}{\mathcal{R}_1(j,j)} & \text{otherwise} \end{cases} \tag{18}$$

$$\mathcal{G}_2(j,j) = \begin{cases} \dfrac{1}{\mathcal{R}_2(j,j)} & |\mathcal{R}_1(j,j)| < |\mathcal{R}_2(j,j)| \\ 1 & \text{otherwise} \end{cases} \tag{19}$$

For the preconditioner $\mathcal{T}$, we use the inverse of the difference between the approximate eigenvalue $\tilde{\omega}$ and the diagonal elements of $\mathcal{H}$, which are given by the orbital energy differences.

From the trial space $\mathcal{Z}$, the analogous set of vectors in the σ-shifted test space is formed:

$$\mathcal{U} = (\mathcal{H} - \sigma\mathcal{M})\mathcal{Z} \tag{20}$$

Again, we can solve the reduced-dimensional generalized eigenvalue problem $(\mathcal{U}^\dagger\mathcal{H}\mathcal{Z}, \mathcal{U}^\dagger\mathcal{M}\mathcal{Z})$ by generalized Schur decomposition, noting that the obtained $\tilde{\omega}_i$ are significantly improved in the region of the eigenspectrum near σ. This yields new factors $\tilde{\mathcal{R}}_1$ and $\tilde{\mathcal{R}}_2$, as well as Schur bases $\tilde{\mathcal{Y}}_\mathrm{L}$, $\tilde{\mathcal{Y}}_\mathrm{R}$. Since the dimension of the eigenproblem in eq 20 is larger than the number of roots that we seek, the eigenvalue−eigenvector pairs are ordered by closeness to the shift value σ, using the standard norm of a complex number given by

$$|(a + bi)| = a^2 + b^2 \tag{21}$$

At this step, it is important to note that the sorting procedure also requires recomputing the factors $\tilde{\mathcal{R}}_1$, $\tilde{\mathcal{R}}_2$, $\tilde{\mathcal{Y}}_\mathrm{L}$, and $\tilde{\mathcal{Y}}_\mathrm{R}$. The matrices $\tilde{\mathcal{R}}_1$ and $\tilde{\mathcal{R}}_2$ are then truncated to the first n columns and n rows to form a new $\mathcal{R}_1$ and $\mathcal{R}_2$. Now we can construct new $\mathcal{V}$, $\mathcal{Q}$ from the left and right Schur bases as

$$\mathcal{V} = \mathcal{Z}\tilde{\mathcal{Y}}_\mathrm{R} \qquad \text{with } \tilde{\mathcal{Y}}_\mathrm{R} \text{ truncated to the first } n \text{ vectors} \tag{22}$$

$$\mathcal{Q} = \mathcal{U}\tilde{\mathcal{Y}}_\mathrm{L} \qquad \text{with } \tilde{\mathcal{Y}}_\mathrm{L} \text{ truncated to the first } n \text{ vectors} \tag{23}$$

In addition, we can store the second set of n vectors (eq 22) in $\mathcal{P}$, to be used on subsequent iterations:

$$\mathcal{P} = \mathcal{Z}\tilde{\mathcal{Y}}_\mathrm{R} \qquad \text{with } \tilde{\mathcal{Y}}_\mathrm{R} \text{ truncated to vectors } n+1 \text{ to } 2n \tag{24}$$

We evaluate the convergence of eigenvectors and continue iterations if necessary. Note that the residual of a trial eigenvector $\mathcal{V}_i$ is given by

$$\mathcal{H}\mathcal{V}_i - \tilde{\omega}_i\mathcal{M}\mathcal{V}_i \tag{25}$$

These residuals are exactly the vectors calculated in the $\mathcal{W}$ block before preconditioning. In addition to evaluating the norm of the residual vector, we also consider a root converged if the change in the eigenvalue is below some (generally lower) threshold.

However, one interesting property of the Davidson algorithm with energy-specific windowing that is not present in GPLHR is the ability to set a hard energy cutoff for converged roots. This

DOI: 10.1021/acs.jctc.8b00141
J. Chem. Theory Comput. 2018, 14, 2034−2041

is often useful to build up a spectrum from multiple calculations on smaller numbers of roots. While basis deflation can also be used to augment the number of vectors,[28] instead of obtaining solutions with energy *greater* than the specified value σ, the solutions could, in principle, all be *less* than σ. Instead, one can also adaptively choose σ such that the n closest vectors are all above the cutoff.

More concretely, if the hard threshold is d, then suppose we start with $\sigma = d$ and let $\omega_1, ..., \omega_n$ be the first n Ritz values with $\omega_i > d$ and ω_0 be the Ritz value closest to σ such that $\omega_0 < d$. Ideally, one should keep σ as close to d as possible to prevent missing any roots. Intuitively, we move σ just far enough to exclude the first Ritz value that is below our chosen threshold, as depicted in Figure 1. That is, calculate the midpoint m of ω_n and ω_0 and use this m as the new σ' if $m > d$, otherwise let $\sigma' = d$. Note that σ is never less than d.

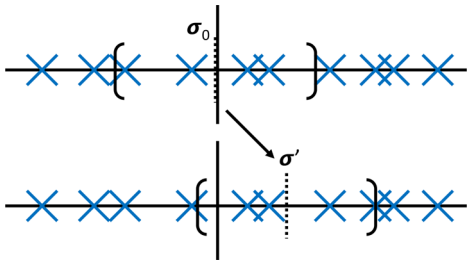

Figure 1. Scheme for adaptive choice of shift value σ. Given some set of Ritz values, we may choose a new σ' to maximize convergence for the first n vectors above a threshold d.

2.3. An Adaptive Davidson/GPLHR Hybrid Algorithm.

The motivation for an adaptive diagonalization algorithm may be best described in analogy to similar techniques used for the SCF procedure and geometry optimization. Quadratically convergent SCF is often too expensive to be used as a method of first choice, but may be employed as a complement to first-order SCF methods on an as-needed basis. Similarly, previous work has found that using a combination of methods for molecular geometry optimization can lead to superior performance.[33] In this work, the development of a hybrid Davidson/GPLHR algorithm is motivated by two considerations: performance and robustness. As mentioned previously, on average, the computational cost of Davidson-like algorithms are less than GPLHR.[29] While the Davidson method provides symmetrized trial vectors that lead to optimal performance in exploring the selected subspace, in the non-Hermitian case, it is possible for the generalized eigenvalue problem to have complex eigenvalues, which leads to a loss of monotonic convergence.[32] Poor approximations in the $\tilde{\omega}_i$ also leads to the generation of new vectors that have little overlap to the true solutions. Without reasonable approximations to the correct eigenvalues, the new vectors generated to augment the subspace are of little value. This is especially common for dense manifolds of states, such as those appearing in the higher-energy X-ray of condensed matter.

On the other hand, GPLHR uses a harmonic Rayleigh–Ritz procedure to locate the eigenvectors with eigenvalues closest to a specified value σ. More-stable convergence is also achieved by transferring additional information about subspace search directions from a block of extra Schur vectors, in contrast to the search direction employed by other methods such as LOBPCG.[34] Despite the algorithmic similarities, GPLHR changes the subspace vectors at each iteration and evaluates their quality systematically by solving the problem in the σ-shifted space. This is in contrast to the Davidson-like procedure, where poor information is not discarded.

In order to switch between the half-dimensional space of eq 6 being used for Davidson and the full space in eq 1, one can take linear combinations of the left $|\mathbf{L}\rangle = |\mathbf{X} - \mathbf{Y}\rangle$ and right $|\mathbf{R}\rangle = |\mathbf{X} + \mathbf{Y}\rangle$ eigenvectors to obtain the $\mathbf{X}$ and the $\mathbf{Y}$ components for some vector $\mathcal{V}$. These vectors are used as the initial "guess" for the GPLHR method. From eq 1, we compute the matrix–vector product for a given trial vector $\begin{pmatrix}\mathbf{X}_i\\ \mathbf{Y}_i\end{pmatrix}$ as

$$\begin{pmatrix}\mathbf{A}\mathbf{X}_i + \mathbf{B}\mathbf{Y}_i\\ \mathbf{B}\mathbf{X}_i + \mathbf{A}\mathbf{Y}_i\end{pmatrix} \tag{26}$$

where we have assumed real orbitals so that $\mathbf{A}^* = \mathbf{A}$ and $\mathbf{B}^* = \mathbf{B}$. It is easy to show that

$$\mathbf{A}\mathbf{X}_i + \mathbf{B}\mathbf{Y}_i = \frac{1}{2}[(\mathbf{A}+\mathbf{B})(\mathbf{X}_i + \mathbf{Y}_i) + (\mathbf{A}-\mathbf{B})(\mathbf{X}_i - \mathbf{Y}_i)] \tag{27}$$

and

$$\mathbf{B}\mathbf{X}_i + \mathbf{A}\mathbf{Y}_i = \frac{1}{2}[(\mathbf{A}+\mathbf{B})(\mathbf{X}_i + \mathbf{Y}_i) - (\mathbf{A}-\mathbf{B})(\mathbf{X}_i - \mathbf{Y}_i)] \tag{28}$$

Construction of the matrix–vector products $(\mathbf{A}+\mathbf{B})(\mathbf{X}+\mathbf{Y})$ and $(\mathbf{A}-\mathbf{B})(\mathbf{X}-\mathbf{Y})$ is accomplished by direct contraction, using the same algorithms as those used for the Davidson method.

The key question for the adaptive scheme is deciding when to switch from the Davidson algorithm to GPLHR. One option is to let the Davidson algorithm run for a set number of iterations and switch if not converged. Similarly, we could switch when the subspace becomes too large and the Davidson algorithm is forced to restart. These are simple to implement and account for at least some situations where convergence was difficult. A more-systematic option is to analyze the convergence behavior itself to determine when subsequent iterations and generated vectors are unlikely to be useful. To do this, we can consider several error metrics. For eigenvalues, we expect the difference in consecutive iterations to go to zero and calculate the norm of the difference vector at iteration i:

$$\delta_i = \left\| \begin{pmatrix}\Delta\omega_1\\ \vdots\\ \Delta\omega_n\end{pmatrix} \right\| \tag{29}$$

The sequence of $\{\delta_i\}$ should be decreasing as we get closer to convergence and provides an overall measure of how close all n roots are to convergence. Note that this is also dependent on the quality of the mapping roots from one iteration to the next. Similarly, for eigenvectors, we expect the residuals, under the action of the RPA matrix, to approach zero.

$$r_i = \|(\mathbf{H} - \mathbf{\Omega}\mathbf{M})\mathcal{V}\| \tag{30}$$

This sequence of $\{r_i\}$ should also approach zero at convergence. In order to determine when to switch, we can examine the sequences of the δ_i and the r_i. If the difference in eigenvalues in consecutive iterations is not decreasing, or equivalently, that enlarging the subspace is not useful, it could be indicative of oscillation or other problems in convergence.

DOI: 10.1021/acs.jctc.8b00141
J. Chem. Theory Comput. 2018, 14, 2034–2041

While it would be tempting to switch immediately if either δ_i or r_i increase, we have found that, even in the case of rather well-behaved systems, the convergence of $\{\delta_i\}$ and $\{r_i\}$ to zero might not be monotonic. To allow for this, we recommend counting the number of iterations in which δ_i or r_i increase and only switch after a set limit is reached.

3. RESULTS AND DISCUSSION

The GPLHR and associated hybrid methods were implemented in a locally modified version of the development version of the Gaussian software package,[35] which includes the energy-specific Davidson method.[8,11−13] All calculations were run using spin-unrestricted density functional theory (DFT) with the B3LYP density functional, unless stated otherwise, and molecular geometries were optimized at the same level of theory.[36,37] Geometries used in benchmarks are given in the Supporting Information. Convergence was determined when either (1) the norm of all the residuals was below a set threshold, $\|r\| < 10^{-5}$, or (2) the change in eigenvalues is less than 10^{-7} Hartrees. All calculations were run on a single compute node with dual Intel Xeon E5-2680 v4 processors for a total of 28 cores and 256 GB DDR3 RAM.

In this first test, we show the agreement of the eigenvalues, and associated eigenvectors found by our GPLHR-based approaches match those given by the energy-specific Davidson algorithm. In Table 1, the first three states of the nitrogen K-edge above 380 eV in NO were computed with the 6-311+G(d) basis set.[38,39] The GPLHR calculation used a subspace expansion parameter of $m = 1$. Note also that, since each GPLHR iteration is roughly 4 times more expensive than a single Davidson iteration, it is performing almost twice as much work in this test case. Although there are very slight differences in excitation energies and oscillator strengths due to numerical differences in convergence, the results of the Davidson and GPLHR algorithms are considered to be identical. Interestingly, at the standard threshold used here, we find that GPLHR gives a better solution than obtained in the Davidson algorithm, as it matches the solution obtained at stricter convergence criteria.

Table 1. Nitrogen K-edge of NO (σ = 380 eV)

ES-Davidson (13 iterations)			GPLHR (7 iterations)		
excitation energy (eV)	oscillator strength (a.u.)	$\langle S^2\rangle$	excitation energy (eV)	oscillator strength (a.u.)	$\langle S^2\rangle$
385.5845	0.0000	2.752	385.5844	0.0000	2.752
386.8976	0.0697	0.753	386.8974	0.0701	0.753
387.3633	0.0341	0.760	387.3632	0.0342	0.760

Generally, for well-behaved RPA problems, such as those for small to moderately sized molecular systems, we found that the Davidson algorithm consistently outperforms GPLHR. This itself is not surprising as GPLHR is designed for much more challenging problems, so that it often does more work than necessary. However, for systems that exhibit a dense manifold of excited states, we find that using GPLHR for some or all iterations is preferred. Two illustrative examples of this are explored here: a graphene sheet and a nanodiamond. In these systems, the carbon K-edge region consists of a dense manifold of C($1s$)→ C($2p$) transitions arising from nearly chemically equivalent carbon atoms. Such scenarios are known to be very challenging for Davidson-like methods.

For a small cluster of graphene sheet (a $C_{28}H_{14}$ structure, as shown in Figure 2), the first 8 states of the carbon K-edge were calculated at the unrestricted B3LYP/6-31G(d)[36,37,40,41] level of theory, using a combination of Davidson and GPLHR iterations. For each calculation, a set number of Davidson iterations were performed first, followed by GPLHR iterations until convergence. In Figure 2, we plot the cumulative number of matrix vector products, since this is the computational bottleneck. The hybrid(n) methods denote a calculation that started using the Davidson algorithm and switched to GPLHR after n iterations. Despite all algorithms converging to the correct roots, the computational cost was least for the hybrid methods. In particular, we note that the hybrid(12) method lead to almost 20% speedup over GPLHR alone, while using only the Davidson algorithm was almost 70% slower. This indicates that there was little benefit of GPLHR over the Davidson algorithm in the first few iterations, and, as a result, extra work was being done. From an algorithmic perspective, this is not too surprising, as the beginning iterations have relatively little information and therefore do not need to be very accurate in extrapolation to provide usable information. Conversely, one of the key reasons why the Davidson type of algorithm struggles here is that it will often include approximate eigenvectors with energies largely dominated by the residual term. This results in new trial vectors being generated that do not aid in capturing the desired region of the spectrum and leads to stagnation. The question that remains is what is a

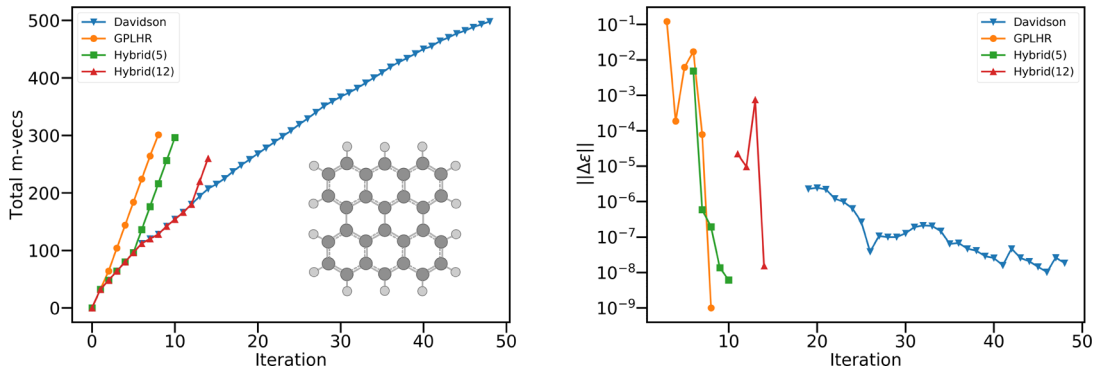

Figure 2. (Left) Cumulative number of matrix vector products performed at each iteration for the energy-specific Davidson, GPLHR, and hybrid methods. Here, Hybrid(n) indicates that n Davidson iterations are performed before switching to GPLHR. The steeper slope of GPLHR indicates that a single iteration is more expensive than a Davidson iteration. (Right) eigenvalue convergence profiles for the fifth root above the threshold, with a vertical excitation energy of 273.468 eV. Iterations before the states could be mapped between iterations are not shown.

DOI: 10.1021/acs.jctc.8b00141
J. Chem. Theory Comput. 2018, 14, 2034−2041

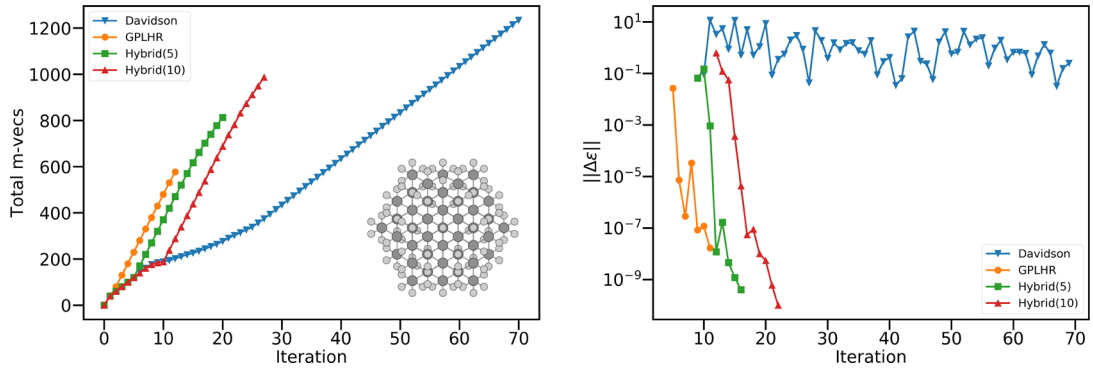

Figure 3. (Left) Cumulative number of matrix−vector products for the $C_{121}H_{104}$ nanodiamond at the 6-31G(d)/UB3LYP level of theory. Hybrid(n) indicates that n Davidson iterations are performed before switching to GPLHR. (Right) eigenvalue convergence profile for the first root above the 260 eV threshold, with a vertical excitation energy of 276.681 eV. Iterations before the states could be mapped between iterations are not shown. Note that the Davidson calculation did not converge within the 70 iterations.

sensible strategy for switching to GPLHR from a Davidson calculation when we do not know a priori how the Davidson algorithm will perform.

The determination of the carbon K-edge spectrum in a nanodiamond cluster was used to test the power of the algorithm on an even larger system. The C_{121} structure is H-capped with 104 H and has C_{3v} symmetry, as shown in Figure 3.[42] The 6-31G(d) basis set[40,41] and B3LYP[36,37] density functional were used for optimization and TDDFT calculations. With 2023 contracted basis functions and 830 total electrons, the dimension of the full RPA matrix is 2 669 280. Of course, the computational bottleneck is the direct formation of the matrix−vector products. The energy-specific Davidson algorithm used with a threshold of 260 eV was unable to converge the first 10 roots after almost 70 iterations, as shown in Figure 3. However, all GPLHR-based hybrid algorithms with σ = 260 eV were able to converge with relative ease. Although the Davidson algorithm is unable to converge this system, forcing the switch to GPLHR on-the-fly also allowed the calculation to be completed successfully. Note that using GPLHR from the beginning would have been optimal for this case; however, the sequences of the error in both the eigenvalues and the residuals show clear signs of problems converging by approximately iteration 5 or 6, using the Davidson method (see Table 2). While it would be impossible to make an optimal general switching rule for all systems, the sequences of error seem to indicate that two or three poor iterations is a reasonable, albeit crude decision metric for detecting breakdown or stagnation. This switching criterion corresponds to the hybrid(5) test shown in Figure 3. At the heart of this problem is the failure to identify the best approximate eigenvectors. Despite the inability of the hybrid method to outperform using the GPLHR algorithm alone on this system, the adaptive hybrid method was nevertheless successful in minimizing the wasted computational effort in the Davidson iterations.

Table 2. Norms of Eigenvalue and Residual Errors at Each Davidson Iteration for the $C_{121}H_{104}$ Nanodiamond at the 6-31G(d)/UB3LYP Level of Theory[a]

iteration	eigenvalue error (a.u.) $\{\delta_i\}$	residual error (a.u.) $\{r_i\}$
1	64.4953	0.00625
2	0.01464	0.00616
3	0.00608	0.00516
4	0.00139	0.00523
5	0.00823	0.11783
6	0.52223	0.08276
7	0.30772	0.27291
8	0.21657	0.00600
9	0.04076	0.08877
10	0.00648	0.09303

[a]The two sequences of $\{\delta_i\}$ and $\{r_i\}$ can be used to determine failure of the Davidson algorithm.

4. CONCLUSION

This paper presents an implementation of a hybrid Davidson−GPLHR algorithm for the solution of the non-Hermitian TDHF/TDDFT equations and explores several modifications. First, since the standard energy-specific Davidson algorithm often performs well, we include the ability to switch to the GPLHR solver on the fly. The additional cost that GPLHR suffers by doing more work than is often necessary for the RPA problem makes it less desirable to use on its own, but it can provide additional robustness for hard-to-converge problems with dense sets of states in the interior of the spectrum. Second, we also include the ability to have the shift value σ adaptively change so that only the first n states above a predefined energy threshold are obtained. This feature is crucial to avoid reconvergence of states when predicting the absorption spectrum over a broader energy range.

Note that, if the matrix can be stored in memory, standard diagonalization routines should always be used. However, this is often not practical for many systems of interest, and one must resort to using iterative direct methods where the matrix−vector products are performed on-the-fly. Adaptive switching between diagonalization methods has the potential to provide superior performance in hard-to-converge eigenvalue problems, including those that are common in X-ray spectroscopy of molecular systems. However, even in cases where using either algorithm alone would be optimal, the adaptive hybrid method provides a reasonable compromise without knowing a priori which one is best.

■ ASSOCIATED CONTENT

Supporting Information

The Supporting Information is available free of charge on the ACS Publications website at DOI: 10.1021/acs.jctc.8b00141.

Cartesian coordinates of molecular systems and calculated transitions (PDF)

DOI: 10.1021/acs.jctc.8b00141
J. Chem. Theory Comput. 2018, 14, 2034−2041

AUTHOR INFORMATION

Corresponding Author

*E-mail: xsli@uw.edu.

ORCID

Joseph M. Kasper: 0000-0002-3840-484X
David B. Williams-Young: 0000-0003-2735-3706
Xiaosong Li: 0000-0001-7341-6240

Notes

The authors declare no competing financial interest.

ACKNOWLEDGMENTS

The development of new eigensolvers for X-ray spectroscopy is funded by the U.S. Department of Energy (No. DE-SC0006863 to X.L.). The application of ab initio spectroscopic methods for studies of nanomaterials is supported by the U.S. National Science Foundation (Nos. CHE-1565520 and CHE-1464497). This research is partially supported by Scientific Discovery through Advanced Computing (SciDAC) program funded by U.S. Department of Energy, Office of Science, Advanced Scientific Computing Research and Basic Energy Sciences, under Contract No. DE-AC02-05CH11231. This work was facilitated though the use of advanced computational, storage, and networking infrastructure provided by the Hyak supercomputer system funded by the STF at the University of Washington and the National Science Foundation (No. MRI-1624430).

REFERENCES

(1) Runge, E.; Gross, E. K. Density-functional Theory for Time-dependent Systems. *Phys. Rev. Lett.* **1984**, *52*, 997−1000.

(2) Casida, M. E. In *Recent Advances in Density Functional Methods (Part I)*; Chong, D., Ed.; World Scientific: Singapore, 1995; p 155.

(3) Petersilka, M.; Gossmann, U.; Gross, E. Excitation Energies From Time-dependent Density-functional Theory. *Phys. Rev. Lett.* **1996**, *76*, 1212−1215.

(4) Davidson, E. R. The Iterative Calculation of a Few of the Lowest Eigenvalues and Corresponding Eigenvectors of Large Real-symmetric Matrices. *J. Comput. Phys.* **1975**, *17*, 87−94.

(5) Weiss, H.; Ahlrichs, R.; Häser, M. A Direct Algorithm for Self-consistent-field Linear Response Theory and Application to C60: Excitation Energies, Oscillator Strengths, and Frequency-dependent Polarizabilities. *J. Chem. Phys.* **1993**, *99*, 1262−1270.

(6) Rettrup, S. An Iterative Method for Calculating Several of the Extreme Eigensolutions of Large Real Non-symmetric Matrices. *J. Comput. Phys.* **1982**, *45*, 100−107.

(7) Coriani, S.; Høst, S.; Jansík, B.; Thøgersen, L.; Olsen, J.; Jørgensen, P.; Reine, S.; Pawłowski, F.; Helgaker, T.; Sałek, P. Linear-scaling Implementation of Molecular Response Theory in Self-consistent Field Electronic-structure Theory. *J. Chem. Phys.* **2007**, *126*, 154108.

(8) Stratmann, R. E.; Scuseria, G. E.; Frisch, M. J. An Efficient Implementation of Time-dependent Density-functional Theory for the Calculation of Excitation Energies of Large Molecules. *J. Chem. Phys.* **1998**, *109*, 8218−8224.

(9) Furche, F. On the Density Matrix Based Approach to Time-Dependent Density Functional Response Theory. *J. Chem. Phys.* **2001**, *114*, 5982−5992.

(10) Dreuw, A.; Head-Gordon, M. Single-reference Ab Initio Methods for the Calculation of Excited states of large molecules. *Chem. Rev.* **2005**, *105*, 4009−4037.

(11) Liang, W.; Fischer, S. A.; Frisch, M. J.; Li, X. Energy-Specific Linear Response TDHF/TDDFT for Calculating High-Energy Excited States. *J. Chem. Theory Comput.* **2011**, *7*, 3540−3547.

(12) Lestrange, P. J.; Nguyen, P. D.; Li, X. Calibration of Energy-Specific TDDFT for Modeling K-edge XAS Spectra of Light Elements. *J. Chem. Theory Comput.* **2015**, *11*, 2994−2999.

(13) Peng, B.; Lestrange, P. J.; Goings, J. J.; Caricato, M.; Li, X. Energy-Specific Equation-of-Motion Coupled-Cluster Methods for High-Energy Excited States: Application to K-edge X-ray Absorption Spectroscopy. *J. Chem. Theory Comput.* **2015**, *11*, 4146−4153.

(14) Ray, K.; DeBeer George, S.; Solomon, E. I.; Wieghardt, K.; Neese, F. Description of the Ground-State Covalencies of the Bis (dithiolato) Transition-Metal Complexes from X-ray Absorption Spectroscopy and Time-Dependent Density-Functional Calculations. *Chem.—Eur. J.* **2007**, *13*, 2783−2797.

(15) Zhang, Y.; Biggs, J. D.; Healion, D.; Govind, N.; Mukamel, S. Core and Valence Excitations in Resonant X-ray Spectroscopy using Restricted Excitation Window Time-dependent Density Functional Theory. *J. Chem. Phys.* **2012**, *137*, 194306.

(16) Lopata, K.; Van Kuiken, B. E.; Khalil, M.; Govind, N. Linear-response and Real-time Time-dependent Density Functional Theory Studies of Core-level Near-edge X-ray Absorption. *J. Chem. Theory Comput.* **2012**, *8*, 3284−3292.

(17) Coriani, S.; Fransson, T.; Christiansen, O.; Norman, P. Asymmetric-Lanczos-chain-driven Implementation of Electronic Resonance Convergent Coupled-cluster Linear Response Theory. *J. Chem. Theory Comput.* **2012**, *8*, 1616−1628.

(18) Fransson, T.; Coriani, S.; Christiansen, O.; Norman, P. Carbon X-ray Absorption Spectra of Fluoroethenes and Acetone: A Study at the Coupled Cluster, Density Functional, and Static-exchange Levels of Theory. *J. Chem. Phys.* **2013**, *138*, 124311.

(19) Kauczor, J.; Norman, P.; Christiansen, O.; Coriani, S. Communication: A Reduced-Space Algorithm for the Solution of the Complex Linear Response Equations used in Coupled Cluster Damped Response Theory. *J. Chem. Phys.* **2013**, *139*, 211102.

(20) Fahleson, T.; Ågren, H.; Norman, P. A Polarization Propagator for Nonlinear X-ray Spectroscopies. *J. Phys. Chem. Lett.* **2016**, *7*, 1991−1995.

(21) Coriani, S.; Christiansen, O.; Fransson, T.; Norman, P. Coupled-Cluster Response Theory for Near-Edge X-ray-Absorption Fine Structure of Atoms and Molecules. *Phys. Rev. A: At., Mol., Opt. Phys.* **2012**, *85*, 022507.

(22) Linares, M.; Stafstrom, S.; Rinkevicius, Z.; Ågren, H.; Norman, P. Complex Polarization Propagator Approach in the Restricted Open-Shell, Self-Consistent Field Approximation: The Near K-Edge X-ray Absorption Fine Structure Spectra of Allyl and Copper Phthalocyanine. *J. Phys. Chem. B* **2011**, *115*, 5096−5102.

(23) Ekström, U.; Norman, P.; Carravetta, V.; Ågren, H. Polarization Propagator for X-ray Spectra. *Phys. Rev. Lett.* **2006**, *97*, 143001.

(24) Fransson, T.; Burdakova, D.; Norman, P. K-and L-edge X-ray Absorption Spectrum Calculations of Closed-shell Carbon, Silicon, Germanium, and Sulfur Compounds Using Damped Four-component Density Functional Response Theory. *Phys. Chem. Chem. Phys.* **2016**, *18*, 13591−13603.

(25) Brabec, J.; Lin, L.; Shao, M.; Govind, N.; Yang, C.; Saad, Y.; Ng, E. G. Efficient Algorithms for Estimating the Absorption Spectrum Within Linear Response TDDFT. *J. Chem. Theory Comput.* **2015**, *11*, 5197−5208.

(26) Van Beeumen, R.; Williams-Young, D. B.; Kasper, J. M.; Yang, C.; Ng, E. G.; Li, X. A Model Order Reduction Algorithm for Estimating the Absorption Spectrum. *J. Chem. Theory Comput.* **2017**, *13*, 4950−4961.

(27) Bauernschmitt, R.; Ahlrichs, R. Treatment of Electronic Excitations Within the Adiabatic Approximation of Time Dependent Density Functional Theory. *Chem. Phys. Lett.* **1996**, *256*, 454−464.

(28) Vecharynski, E.; Yang, C.; Xue, F. Generalized Preconditioned Locally Harmonic Residual Method for Non-Hermitian Eigenproblems. *SIAM J. Sci. Comp.* **2016**, *38*, A500−A527.

(29) Zuev, D.; Vecharynski, E.; Yang, C.; Orms, N.; Krylov, A. I. New Algorithms for Iterative Matrix-free Eigensolvers in Quantum Chemistry. *J. Comput. Chem.* **2015**, *36*, 273−284.

DOI: 10.1021/acs.jctc.8b00141
J. Chem. Theory Comput. 2018, 14, 2034−2041

(30) Vecharynski, E.; Brabec, J.; Shao, M.; Govind, N.; Yang, C. Efficient Block Preconditioned Eigensolvers for Linear Response Time-dependent Density Functional Theory. *Comput. Phys. Commun.* **2017**, *221*, 42−52.
(31) Olsen, J.; Jensen, H. J. A.; Jørgensen, P. Solution of the Large Matrix Equations Which Occur in Response Theory. *J. Comput. Phys.* **1988**, *74*, 265−282.
(32) Kauczor, J.; Jørgensen, P.; Norman, P. On the Efficiency of Algorithms for Solving Hartree−Fock and Kohn−Sham Response Equations. *J. Chem. Theory Comput.* **2011**, *7*, 1610−1630.
(33) Li, X.; Frisch, M. J. Energy-Represented Direct Inversion in the Iterative Subspace Within a Hybrid Geometry Optimization Method. *J. Chem. Theory Comput.* **2006**, *2*, 835−839.
(34) Knyazev, A. V. Toward the Optimal Preconditioned Eigensolver: Locally Optimal Block Preconditioned Conjugate Gradient Method. *SIAM J. Sci. Comput.* **2001**, *23*, 517−541.
(35) Frisch, M. J.; Trucks, G. W.; Schlegel, H. B.; Scuseria, G. E.; Robb, M. A.; Cheeseman, J. R.; Scalmani, G.; Barone, V.; Petersson, G. A.; Nakatsuji, H.; Li, X.; Caricato, M.; Marenich, A. V.; Bloino, J.; Janesko, B. G.; Gomperts, R.; Mennucci, B.; Hratchian, H. P.; Ortiz, J. V.; Izmaylov, A. F.; Sonnenberg, J. L.; Williams-Young, D.; Ding, F.; Lipparini, F.; Egidi, F.; Goings, J.; Peng, B.; Petrone, A.; Henderson, T.; Ranasinghe, D.; Zakrzewski, V. G.; Gao, J.; Rega, N.; Zheng, G.; Liang, W.; Hada, M.; Ehara, M.; Toyota, K.; Fukuda, R.; Hasegawa, J.; Ishida, M.; Nakajima, T.; Honda, Y.; Kitao, O.; Nakai, H.; Vreven, T.; Throssell, K.; Montgomery, J. A., Jr.; Peralta, J. E.; Ogliaro, F.; Bearpark, M. J.; Heyd, J. J.; Brothers, E. N.; Kudin, K. N.; Staroverov, V. N.; Keith, T. A.; Kobayashi, R.; Normand, J.; Raghavachari, K.; Rendell, A. P.; Burant, J. C.; Iyengar, S. S.; Tomasi, J.; Cossi, M.; Millam, J. M.; Klene, M.; Adamo, C.; Cammi, R.; Ochterski, J. W.; Martin, R. L.; Morokuma, K.; Farkas, O.; Foresman, J. B.; Fox, D. J. *Gaussian Development Version, Revision I.10++*. Gaussian, Inc.: Wallingford, CT, 2016.
(36) Becke, A. Density Functional Thermochemistry. III. The Role of Exact Exchange. *J. Chem. Phys.* **1993**, *98*, 5648−5652.
(37) Stephens, P. J.; Devlin, F. J.; Chabalowski, C. F.; Frisch, M. J. Ab Initio Calculation of Vibrational Absorption and Circular Dichroism Spectra Using Density Functional Force Fields. *J. Phys. Chem.* **1994**, *98*, 11623−11627.
(38) Krishnan, R.; Binkley, J. S.; Seeger, R.; Pople, J. A. Self-consistent Molecular Orbital Methods. XX. A Basis Set for Correlated Wave Functions. *J. Chem. Phys.* **1980**, *72*, 650−654.
(39) Clark, T.; Chandrasekhar, J.; Spitznagel, G. W.; Schleyer, P. V. R. Efficient Diffuse Function-augmented Basis Sets for Anion Calculations. III. The 3-21+ G Basis Set for First-row Elements, Li−F. *J. Comput. Chem.* **1983**, *4*, 294−301.
(40) Hariharan, P. C.; Pople, J. A. The Influence of Polarization Functions on Molecular Orbital Hydrogenation Energies. *Theor. Chem. Acc.* **1973**, *28*, 213−222.
(41) Francl, M. M.; Pietro, W. J.; Hehre, W. J.; Binkley, J. S.; Gordon, M. S.; DeFrees, D. J.; Pople, J. A. Self-consistent Molecular Orbital Methods. XXIII. A Polarization-type Basis Set for Second-row Elements. *J. Chem. Phys.* **1982**, *77*, 3654−3665.
(42) Petrone, A.; Goings, J. J.; Li, X. Quantum Confinement Effects on Optical Transitions in Nanodiamonds Containing Nitrogen Vacancies. *Phys. Rev. B: Condens. Matter Mater. Phys.* **2016**, *94*, 165402.

DOI: 10.1021/acs.jctc.8b00141
J. Chem. Theory Comput. 2018, 14, 2034−2041